New Solids Based on $B_{12}N_{12}$ Fullerenes

J. M. Matxain*

Department of Natural Sciences and Örebro Life Sciences Center, Örebro University, 70182 Örebro, Sweden, Kimika Fakultatea, Euskal Herriko Unibertsitatea, P.K. 1072, 20018 Donostia, Euskadi, Spain, and Donostia International Physics Center, 20080 Donostia, Euskadi, Spain

L. A. Eriksson

Department of Natural Sciences and Örebro Life Sciences Center, Örebro University, 70182 Örebro, Sweden

J. M. Mercero, X. Lopez, M. Piris, and J. M. Ugalde

Kimika Fakultatea, Euskal Herriko Unibertsitatea, P.K. 1072, 20018 Donostia, Euskadi, Spain, and Donostia International Physics Center, 20080 Donostia, Euskadi, Spain

J. Poater

Afdeling Theoretische Chemie, Scheikundig Laboratorium der Vrije Universiteit, De Boelelaan 1083, NL-1081 HV Amsterdam, The Netherlands

E. Matito and M. Solà

Institut de Quimica Computacional, Departament de Quimica, Universitat de Girona, 17071 Girona, Catalonia, Spain

Received: May 16, 2007; In Final Form: July 4, 2007

In recent years, BN fullerenes have been synthesized experimentally. As their carbon counterparts, these BN fullerenes could be assembled in molecular solids, but this possibility has been studied little in the literature. In this work, we focus on the smallest synthesized BN fullerene, $B_{12}N_{12}$, which is built by squares and hexagons. First, the interaction between two of these fullerenes has been analyzed, using the hybrid B3LYP and MPW1PW91 density functional methods. Two different interactions have been studied in the dimer, a square facing a square (S−S) and a hexagon facing a hexagon (H−H). In both cases, a B is facing a N. The most stable dimer was found to be S−S facing, with covalent interactions between the monomers, but other dimers with weak interactions have been found as well, which opens possibilities of new systems, as in the case of fullerene dimers and solids. The solids resulting from the infinite repetition of the characterized dimers were optimized, finding two different solids, with covalent and weak interactions between monomers, respectively. The solid with covalent interactions is a nanoporous material that is more stable by around 12 eV. Because of the nanoporous character of this solid, it could be used for heterogeneous catalysis, molecular transport, and so forth. The SIESTA code with the GGA-PBE density functional method has been used for the solid-state calculations.

I. Introduction

Over 40 years ago, Richard Feynman described how in nanotechnology "there is plenty of room at the bottom!".[1] Indeed, the recent spectacular growth of nanotechnology has followed the predictions of some of the pioneers in the field, such as Arthur von Hippel[2] and K. Eric Drexler.[3,4] There have been many important developments in nanotechnology[5−8] and new and revolutionary techniques have been developed, such as the scanning tunneling microscope (STM), the atomic force microscope (AFM), and others. It might be possible to create new materials which are useful in a broader sense than their bulk counterparts.[9−13] The recent spectacular success of nanotechnology makes cluster science very interesting, since, in addition to rationalizing some surface-related and other properties of bulk materials, studies of clusters of increasingly larger sizes can eventually bridge the gap with nanosize materials in a comprehensible manner. Consequently, the literature in the field is growing rapidly, and several reviews of cluster science have appeared.[14−16] One of the best known class of clusters or nanostructures are the so-called fullerenes discovered in 1985[17] which are hollow carbon spheroidal structures.

Interest in fullerene valence isoelectronic clusters such as III−V clusters is also growing rapidly. Studies of small III−V clusters have become routine works in the literature,[18−21] along with studies of large clusters or bulk material.[22−24] III−V fullerenes and nanotubes have also been studied.[25−28] Concretely, B_iN_i structures have been widely studied both theoretically and experimentally. Theoretical studies have been performed for fullerene-like $B_{12}N_{12}$ clusters,[29,30] where it has been found that a structure built from squares and hexagons is more

* Corresponding author. E-mail: jonmattin.matxain@ehu.es.

10.1021/jp073773j CCC: $37.00
Published on Web 08/18/2007

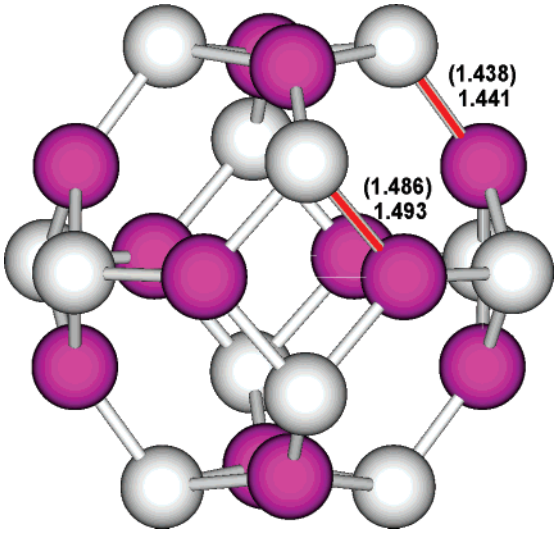

Figure 1. Optimized $B_{12}N_{12}$ fullerene structure with T_h symmetry. Distances calculated using B3LYP and MPW1PW91, in brackets, are given in Å.

stable than those built from pentagons and hexagons. This is due to the fact that in the second case less stable B−B and N−N bonds are formed. The most stable $B_{12}N_{12}$ structure is built from six squares and eight hexagons. This structural pattern has also been found by Wu et al.,[31] who also studied larger B_iN_i clusters, $i = 12$, 20, 22, 24, 26, 28, 30, 32, 34, and 36. Other theoretical calculations have focused on searching for the global minima structures for small B_iN_i clusters, $i = 2-15$ by Matxain et al.[32] and $i = 13$, 14, and 16 by Strout.[33] Both studies agree, predicting spheroid structures built by squares and hexagons to be the global minima for $i > 11$. $B_{12}N_{12}$, built by six squares and eight hexagons, is the smallest high-symmetric global minimum. The $B_{36}N_{36}$ fullerene was also studied previously,[34] and a structure built from six squares and 32 hexagons was been found. Experimentally, small BN clusters have been characterized recently by Oku and co-workers, supporting previous theoretical predictions. In addition, mixed experimental and theoretical studies of $B_{12}N_{12}$,[35] $B_{24}N_{24}$,[36−38] $B_{28}N_{28}$,[39] and B_iN_i $i = 24-60$[40] have appeared in the last years. Moreover, the nitrogen NMR chemical shifts of some of these structures have been calculated theoretically by Barone et al.[41]

Similar structural trends have been observed for II−VI clusters.[42,43] In general, the number of rings appearing in the different heteroatomic X_iY_i cluster structures can be predicted by the simple rules obtained from Euler's law:

$$N_{6-\text{ring}} = i - 4 - 2N_{8-\text{ring}} \qquad N_{4-\text{ring}} = 6 + N_{8-\text{ring}} \quad (1)$$

which states that in a closed structure formed by polyhedra, the number of vertexes plus the number of faces will always equal the number of edges plus 2.

Carbon fullerenes interact with each other to form molecular solids, the so-called fullerites. The interactions between the fullerenes in these solids are very weak, and the fullerene structure does not change. Carbon fullerenes and BN clusters are isoelectronic, and as both are known to form fullerenes, it could be argued that BN clusters could form these types of solids as well. In this work, we focus on the $B_{12}N_{12}$ spheroid and its capability to form dimers and solids. In a recent work,[44] Prokovitny has explained the structure of the boron nitride E phase as a solid built by $B_{12}N_{12}$ fullerenes. This boron nitride phase was first synthesized by Batsanov et al. in 1965,[45] by the explosive shock compression of turbostratic boron nitride. It was named as E phase or E-BN because of the method used in its synthesis. Later, this structure was synthesized by other experimental techniques as well, but the structure of this new phase was not correctly modeled, until Prokovitny's work. In this structure, $B_{12}N_{12}$ form covalent bonds with other fullerenes, forming a rhombic structure. Other covalent crystals based on $B_{12}N_{12}$ fullerenes were also predicted earlier by Prokovitny et al.,[46] whose crystal structure was cubic, with simple cubic (sc), body-centered cubic (bcc), and face-centered cubic (fcc) lattices.

Our aim is to study the interaction between $B_{12}N_{12}$ clusters as the basis for molecular solid formation, being the interaction between $B_{12}N_{12}$ fullerenes of the van der Waals type and not covalent as in the Prokovitny structures. Different systems and orientations were explored using the geometries characterized in a previous work,[32] that is, squares facing squares (S−S) and hexagons facing hexagons (H−H). Once the most stable dimer structure was found, the geometries obtained were used as a starting point for optimizing the molecular solid structure, where the dimer is the unit cell, and both intra- and intercell parameters are optimized. In this way, a new BN crystal structure, of van der Waals type, is characterized.

II. Methods

In order to calculate the interaction energy curves for the dimers, monomer geometries as characterized in ref 32 were used. Since these monomers are built from squares and hexagons, two different ways of interaction have been studied, namely, S−S and H−H. In both cases, a N on one monomer is facing a B on the other, forming a dative N−B bond. Two exchange-correlation functionals have been used, within the density functional theory (DFT) framework.[47] On one hand was the hybrid Becke 3 Lee-Yang-Perdew (B3LYP) gradient-corrected approximation,[48,49] and on the other hand was the hybrid one parameter functional using modified Perdew−Wang exchange and Perdew−Wang 91 correlation (MPW1PW91).[50] This functional was parametrized to calculate correctly weak interactions as noble gas dimers. These two functionals were chosen because in previous studies of B−N dative bonds it was observed that MPW1PW91 provided accurate results while B3LYP yielded poor results.[51,52] However, in those studies, MP2[53] was the most tried method. We have also performed MP2 calculations when possible, because of the large size of our dimer. Soft pseudopotentials[54] were used to model the core electrons. These were combined with an efficient uncontracted Gaussian basis set for the valence electrons, consisting on five s type, five p type, and one d type functions for both B and N.[32] It was demonstrated[32] that this combination of pseudopotential and basis set provides accurate results. All of these dimer calculations were carried out using the GAUSSIAN03 program package.[55]

To explore possible molecular solids constructed from the $B_{12}N_{12}$ dimer, we performed DFT calculations using the SIESTA computer code.[56] Exchange and correlation effects were described using the generalized gradient approximation (GGA), within the Perdew−Burke−Ernzerhof (PBE) functional.[57] This functional has shown to provide reasonably good results for dative B−N bonds,[51,52] with its performance lying in between MPW1PW91 and B3LYP but much better than the last one. Core electrons were replaced by Troullier−Martins norm-conserving pseudopotentials[58] in the Kleinman−Bylander factorized form.[59] In the context of Siesta, the use of pseudopotentials imposes basis orbitals adapted to them. Furthermore, SIESTA employs a localized basis set to represent the Kohn−Sham orbitals for valence electrons. Accordingly, the basis set

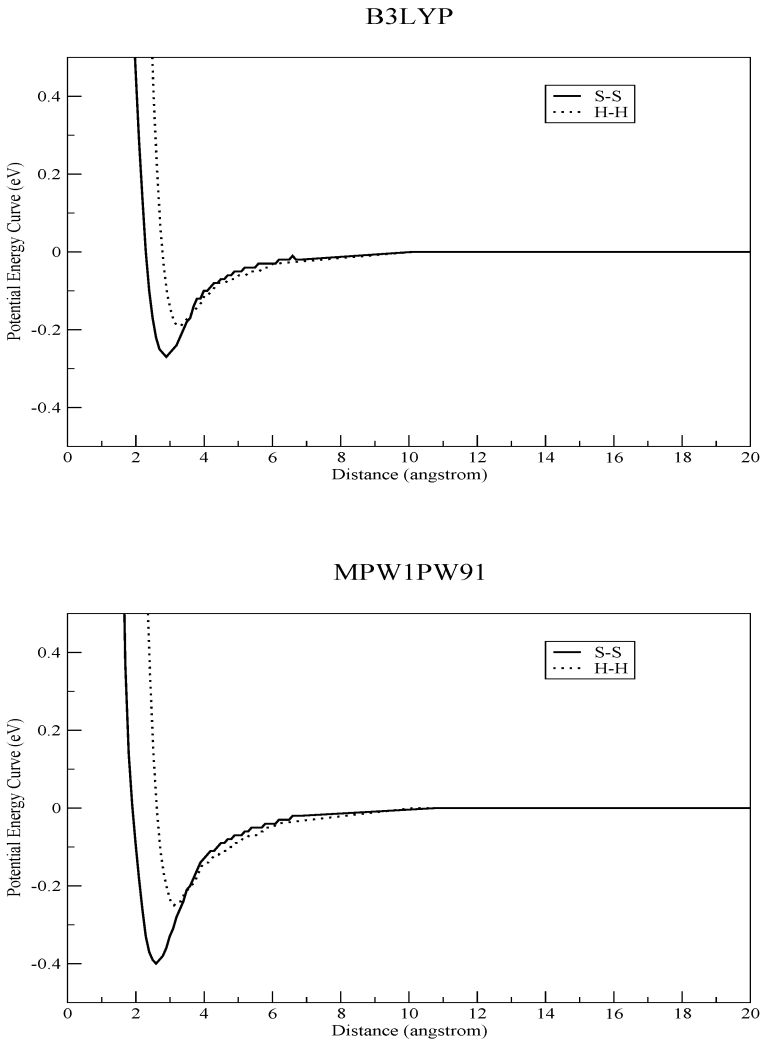

Figure 2. Potential energy curves (in eV) for $B_{12}N_{12}$ fullerene dimers, as a function of the distance between rigid monomers, calculated for both S−S and H−H Facing, using the B3LYP (up) and MPW1PW91 (down) functionals.

of atomic orbitals is constructed from numerical solutions of the atomic pseudopotential and are constrained to be zero beyond a cutoff radius. We used one basis set of double ζ plus polarization quality (DZP). The single parameter (orbital energy shift) that defines the confinement radii of different orbitals was $\Delta E_{PAO} = 150$ meV, which gives typical precision within the accuracy of the used GGA functional. With this basis set, SIESTA calculates the self-consistent potential on a grid in real space. The fineness of this grid is determined in terms of an energy cutoff in analogy to the energy cutoff when the basis set involves plane waves. In our calculations, we used an equivalent plane wave cutoff energy of 200 Ry. In every case, the geometry was relaxed until the maximum forces were smaller than 0.04 eV/Å. In the solid-state calculation, periodic boundary conditions were employed considering a k mesh according to the Monkhorst−Pack[60] scheme ($10 \times 10 \times 10$).

III. Results

In section III.1, the obtained interaction energy curves and properties of optimized $B_{12}N_{12}$ spheroid dimers are given. In section III.2, the study of the solids based on different possible dimers is performed.

1. Stability of Different $B_{12}N_{12}$ Fullerene Dimers. The $B_{12}N_{12}$ spheroids are built by eight hexagons and six squares, as may be observed in Figure 1. The symmetry of this fullerene is very high, T_h, and the squares are placed in such a way that they fit with the Cartesian axes *x*, *y*, and *z*. Within squares, the bond distances are a bit larger than out of the squares, 1.493 Å versus 1.441 Å, calculated at the B3LYP level of theory.

In general, a significant difference between the BN fullerene and the carbon fullerenes is that BN fullerenes are composed from two different atoms. N has a lone pair pointing out from the surface of the spheroid, while B has an empty orbital. Thus, dimers containing B facing N would be more stable than those having N to N, because of the repulsion between the two lone pairs. On the basis of the fact that the spheroids are built by squares and hexagons, the most stable dimer orientations will be H−H or S−S. In addition to this, regarding the similarities with isoelectronic carbon fullerenes, one may think that the interaction between the two monomers is weak. However, previous works reporting covalent crystals built by $B_{12}N_{12}$ fullerenes[46] show covalent bonds between monomers, with no loss of the structure of the monomers. In this work, we have checked all possible dimer interactions, named as Cov_{S-S} and

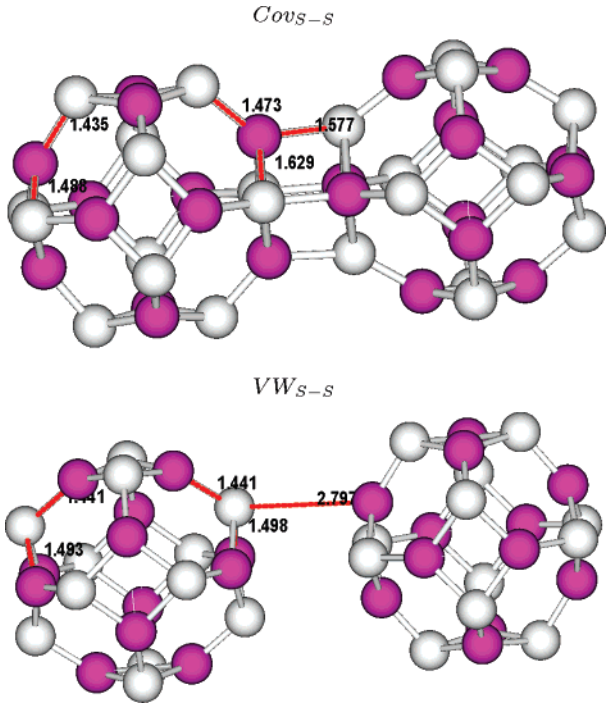

Figure 3. Optimized structures of the calculated square−square $B_{12}N_{12}$ fullerene dimers, namely, *Cov*$_{S-S}$, top and *VW*$_{S-S}$, bottom.

Cov_{H-H} for covalent interactions facing squares and hexagons, respectively, and VW_{S-S} and VW_{H-H} for weak van der Waals interactions facing squares and hexagons, respectively. All of these possible interactions have been studied using two different functionals, B3LYP and MPW1PW91. The latter was parametrized for describing the van der Waals interactions in nobel gas dimers.

In a first attempt to study these interactions, we have considered each monomer as a rigid molecule; that is, the structure of each monomer remains unaltered, and the energy has been calculated as a function of the distance between each monomer. This is a good approach to the problem, since one expects the structure of each monomer not to change very much, to retain its identity. The potential energy curves for S−S and H−H facing, ranging from 1 to 20 Å, are depicted in Figure 2. Both B3LYP and MPW1PW91 predict, surprisingly, S−S interaction to be more stable than H−H interaction, although in the latter case there are more B···N interactions that could stabilize the dimer. In the S−S case, the interaction energy is 0.08 eV more stable than the H−H case, calculated with B3LYP, and 0.15 eV more stable according to MPW1PW91. In addition to this, MPW1PW91 also predicts larger dissociation energies, 0.40 eV for the S−S and 0.25 eV for the H−H cases, in contrast with the 0.27 and 0.19 eV calculated by B3LYP. About the equilibrium distances, the S−S bond distances are much shorter than the H−H ones, 0.4 and 0.5 Å, according to B3LYP and MPW1PW91, respectively. However, MPW1PW91 predicts shorter distances than B3LYP by around 0.2 Å.

The potential energy curves, calculated with rigid monomers, do not predict covalent interaction between the monomers. This may be due to the fact that the rigidity of the monomers do not favor appropriate angles for covalent bonding. We have fully optimized the dimer structures (Figure 3) using as starting points the minima of the curves obtained in Figure 2. When the monomers are allowed to relax in the dimer, not only the weak dimers are obtained, but also the covalent Cov_{S-S} dimer is obtained. However, all attempts to locate the Cov_{H-H} dimer, using both B3LYP and MPW1PW91, lead to a condensed $B_{24}N_{24}$ cluster. This fact is in discordance with the findings about the E-BN phase, by Prokovitny.[44] He proposed a structure where the $B_{12}N_{12}$ fullerenes were covalently bonded by the hexagons, but according to our calculations, these structures probably would collapse in other structures. All energetics and geometrical parameters of isolated monomers and optimized dimers are given in Table 1.

TABLE 1: Bond-Distances in Angstroms[a]

	$R_{Mon-Mon}$	R^a_{B-N}	R^b_{B-N}
Cov$_{S-S}$	1.583 (1.577)	1.645 (1.629)	1.494 (1.488)
VW$_{S-S}$	2.797 (2.760)	1.498 (1.492)	1.493 (1.486)
VW$_{H-H}$	3.274 (3.131)	1.494 (1.488)	1.493 (1.486)
	ΔE	ΔE_0	ΔG
Cov$_{S-S}$	0.0 (0.0)	0.0 (0.0)	0.0 (0.0)
VW$_{S-S}$	1.50 (2.07)	1.52 (2.07)	1.46 (2.06)
VW$_{H-H}$	1.56 (2.17)	1.61 (2.21)	1.44 (2.05)

[a] $R_{Mon-Mon}$ stands for the distance between monomers; R^a_{B-N} is the B−N distance within the interacting ring of the monomer; and R^b_{B-N} is the B−N distance but in the ring opposite to the interaction. Relative electronic energies (ΔE), corrected with zero-point vibrational energies (ΔE_0), and Gibbs free energies (ΔG), with respect to the most stable dimer, in eV. Out of the brackets, the B3LYP values are given, and in brackets, the MPW1PW91 values are given.

Both B3LYP and MPW1PW91 yield similar results for the geometries. In the covalent dimer, the geometries of the monomers suffer a small change in the interaction region. Thus, the B−N bond lengths are enlargered about 0.10−0.15 Å, comparing the values of R^a_{B-N} with the values of the isolated monomer given in Figure 1. This distortion only occurs in the interaction region, since the values of the rings located opposite to the interaction remain very similar to those of the isolated monomer. This change in the bond length makes possible a relaxed interaction between the monomers, and it is crucial for the formation of covalent bonds between the monomers. As one could expect, the covalent interactions are more stable than the van der Waals interactions. In the case of the S−S facing, the covalent dimer is 1.50 and 2.07 eV more stable than the van der Waals dimer, according to B3LYP and MPW1PW91, respectively. The VW_{H-H} dimer is less stable than the VW_{S-S} dimer, according to the ΔE and ΔE_0, but when one takes into account the entropy, the VW_{H-H} dimer becomes more stable by 0.02 and 0.01 eV, according to B3LYP and MPW1PW91, respectively.

The energy differences between covalent and van der Waals dimers are rather large. However, to calculate properly the relative stability of van der Waals dimers, the energy barrier with respect to the covalent dimers and the depth of the van der Waals dimers should be calculated. This depth has been already calculated in the potential energy curves of rigid monomers, since it was observed that the geometries of the monomers in the van der Waals dimers were very similar to those of the isolated monomers. Recall that the dissociation energies were calculated to be 0.40 eV for VW_{S-S} and 0.25 eV for VW_{H-H}, according to MPW1PW91, and 0.27 and 0.19 eV calculated by B3LYP. The dissociation energies are sufficiently large to ensure that the dimer will not dissociate at room temperature. To calculate the energy barriers to cross from covalent to van der Waals dimers, scan calculations have been performed for the S−S case. In these calculations, the $R_{Mon-Mon}$ distance is fixed for several distances, and the remaining parameters are optimized. In this way, we can find the maximum in the potential energy curve that determines the transition state, and the energy barriers can be calculated. The calculated scan

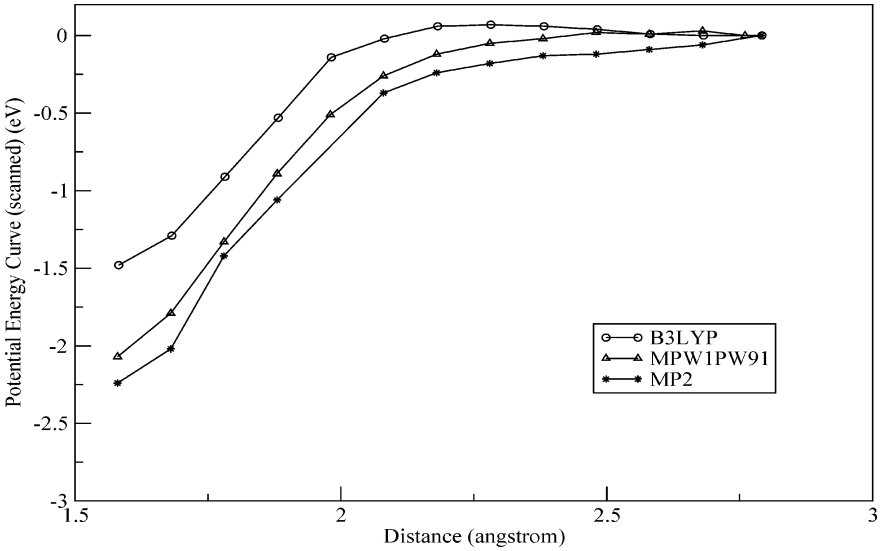

Figure 4. Scanned potential energy curves (eV) for $B_{12}N_{12}$ fullerene dimers, as a function of the distance between monomers, calculated from the Cov_{S-S} to the VW_{S-S} dimer, using the B3LYP and MPW1PW91 functionals.

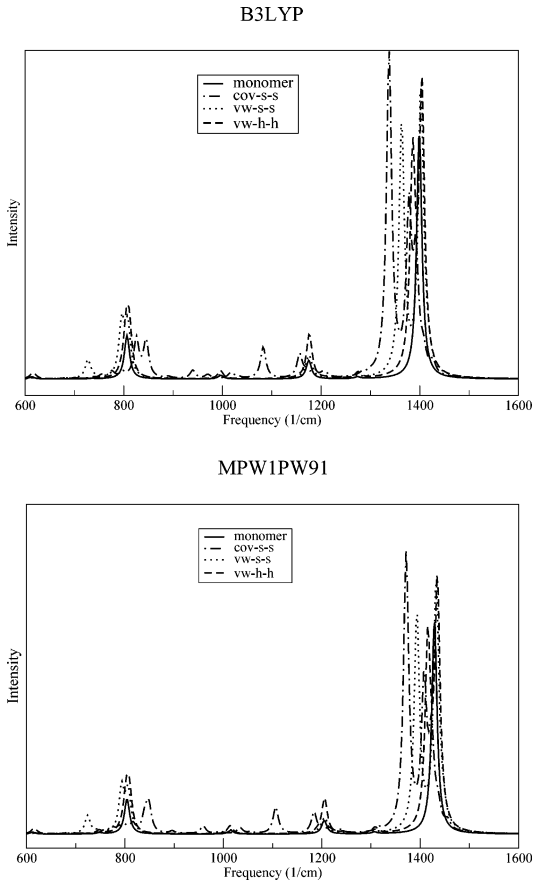

Figure 5. IR spectra of the characterized $B_{12}N_{12}$ fullerene dimers, calculated using B3LYP (top) and MPW1PW91 (bottom), compared with the monomer IR data.

curves are depicted in Figure 4. One may observe that both B3LYP and MPW1PW91 predict small barriers, the last one being almost barrierless, while MP2 calculations do not show any barrier at all. In fact, this shows that the van der Waals dimer is not very stable. It is very likely that the mean lifetime of the van der Waals dimer is very short.

What are the vibrational modes corresponding to the dimers? Do they differ from the monomer's spectrum? Are they very different for different dimers? In Figure 5 the IR spectra of all characterized dimers are given, compared with the $B_{12}N_{12}$ monomer IR spectrum. Having a look at the MPW1PW91 data, we may observe three picks for the monomer, at 806.6, 1175.1, and 1399.0 cm^{-1}, respectively. For B3LYP, the results are very similar, and for further discussion, the MPW1PW91 data will be used. According to the IR spectra, the van der Waals dimers have very similar spectra compared to the regular dimer. However, the covalent dimer has a slightly different spectra.

TABLE 2: Lattice Constant, *a*, and Bond-Distances, in Å[a]

	a	$R_{Mon-Mon}$	R^a_{B-N}	R^b_{B-N}	B_e	ΔE
Cov_{S-S}	11.80	1.575	1.617	1.617	−2.04	0.0
VW_{S-S}	13.28	2.518	1.503	1.503	−14.08	12.04

[a] $R_{Mon-Mon}$ stands for the distance between monomers; R^a_{B-N} is the B−N distance within the interacting ring of the monomer; and R^b_{B-N} is the B−N distance but in the ring opposite to the interaction.

2. Electronic Structure and Properties of Covalent and van der Waals $B_{12}N_{12}$ Solids. The unit cells of both covalent and van der Waals solids are defined to be the S−S faced $B_{12}N_{12}$ fullerene dimer. The need of including the dimer in the unit cell instead of the monomer comes from the fact that a B from a monomer must face a N. It is not possible to build this situation only with the translation of the monomer, and therefore, the dimer must be included in the unit cell. In this way, the translation vectors are defined to be 0.5, 0.5, and 1, being one in the direction of the dimer interaction. In this way, we ensure that each monomer's B faces a N and not another B. The difference between the unit cell of the covalent solid and the van der Waals solid is the intermonomer distance. To start with, the distances found in the optimized dimers have been used. This building block has a symmetric shape. The centers of $B_{12}N_{12}$ molecules favor the bulk fcc structure, with a nearest-neighbor distance that corresponds to the diameter of the molecule. The fcc structure has been experimentally observed in the valence isoelectronic crystalline C_{60}, in which each Bravais-lattice site is occupied by a single fullerene molecule.

In Table 2, the geometrical and energetic values of the two characterized solids are given. Having a look at the geometrical parameters, we find our calculations reveal that the lattice parameter of the cubic unit cell of the van der Waals solid is 13.28 Å, with the distance between the monomers 2.518 Å. Compared with the VW_{S-S} dimer, the distance has been lowered by approximately 0.25 Å, but the van der Waals character of the interaction is clear. The distances inside each monomer are

Figure 6. Solid structure of the covalently bonded fcc solid of $B_{12}N_{12}$ fullerenes.

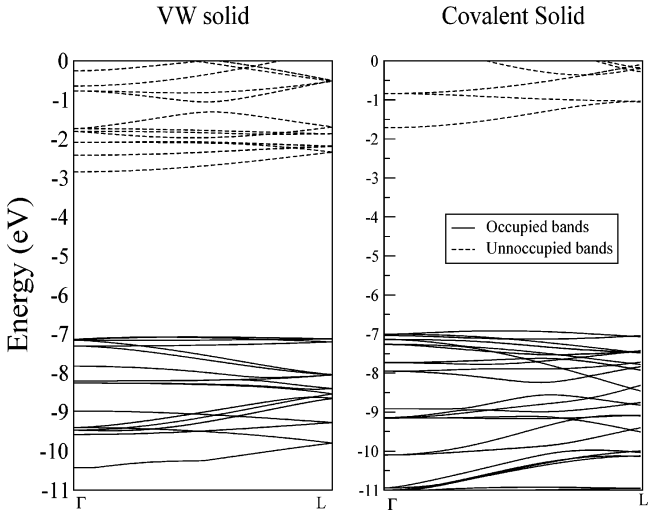

Figure 7. Band structure for the calculated $B_{12}N_{12}$ van der Waals and covalent fcc solids.

very similar to those of the isolated monomer, as one could expect from the weak interaction. On the other hand, the lattice parameter of the cubic unit cell of the covalent solid is about 2 Å smaller, with the distance between the monomers 1.5 Å. This shortening of the distance has a small distortion in the monomer, where the distances inside increase by 0.15 Å, as happened in the Cov_{S-S} dimer. This covalent solid is a nanoporous material, as can be observed in Figure 6, which could be useful in a number of different fields like heterogeneous catalysis, molecular transport, and so forth. The Cartesian coordinates of the optimized unit cells of both solids, along with the cell vectors and other structural parameters, are available in Supporting Information.

The binding energies for the two crystal structures are 14.33 and 2.28 eV, for the covalent and the van der Waals solids, respectively. As expected, the binding energy of the covalent solid is larger than the van der Waals one. In section III.1, we estimated that the there was no energy barrier to move from the VW_{S-S} dimer to the Cov_{S-S} dimer, and therefore, one may think that the relative stability of the van der Waals solid could be very small, unless it is stabilized somehow.

Finally, the band structure of the two predicted solids has been studied, and the results obtained are plotted in Figure 7. In the solid state, the overlap of orbitals broadens the levels to bands. Our calculations predict both $B_{12}N_{12}$ solids to be insulators. The indirect gaps are of 5.20 and 4.23 eV, for the covalent and VW solids, while the direct gaps at Γ point are 5.29 and 4.29 eV. The widths of the highest occupied bands are 0.14 and 0.06 eV for covalent and VW solids, respectively, and the lower-lying bands show appreciable dispersion up to 0.75 eV. Bandwidths of 0.67 and 0.5 eV are obtained for the lowest unoccupied molecular orbital (LUMO) bands of covalent and VW solids, respectively. These band gaps are significantly lower than the highest occupied molecular orbital (HOMO)−LUMO gap of the monomers, which is 6.78 eV.

IV. Conclusions

$B_{12}N_{12}$ cluster is built by squares and hexagons. The most stable dimers therefore may be S−S or H−H. In this work, four different $B_{12}N_{12}$ dimers have been studied, Cov_{S-S}, Cov_{H-H}, VW_{S-S}, and VW_{H-H}, where Cov stands for covalent dimers and VW stands for van der Waals dimers. Among these tried four dimers, only three have been found to be stable, Cov_{S-S}, VW_{S-S}, and VW_{H-H}. The Cov_{H-H} converge to a $B_{24}N_{24}$ monomer. In the VW dimers, the monomer distortion is very small, but in the Cov dimer, the B−N distance within the monomer increases by 0.15 Å nearby the interaction region. Nevertheless, each monomer keeps its structure unaltered in all cases. Comparing the two VW interactions, it is observed that the VW_{S-S} is more stable. The bond length is 0.5 Å shorter, and the dissociation energy is about 0.16 eV more stable. Comparing the Cov_{S-S} and the VW_{S-S}, we observe that the covalent dimer is more stable, around 1.6 eV. The VW dimers IR are very similar to that of the monomer; only the covalent dimer has a significantly different IR spectrum.

With the characterized dimers, two solids have been characterized, the Cov_{S-S} and the VW_{S-S} solids. In both cases, the fcc structure is favored. The distances between monomers are 1.5 and 2.5 Å for covalent and van der Waals solids, respectively, in good agreement with dimer geometries. As the dimer, the Cov_{S-S} solid is more stable than the VW_{S-S} solid by 12.04 eV. The band analysis of both solids reveal that both solids are insulators.

Acknowledgment. This research was funded by the Swedish National Research council and the Government of the Basque Country (SAIOTEK program) and the Ministerio de Educacion y Ciencia. The SGI/IZO-SGIker UPV/EHU (supported by Fondo Social Europeo and MCyT) is gratefully acknowledged for the generous allocation of computational resources. This paper is dedicated to the memory of Professor Lorenzo Pueyo, an inspiring colleague.

Supporting Information Available: Optimized unit cell and lattice vectors. This material is available free of charge via the Internet at http://pubs.acs.org.

References and Notes

(1) Feynmann, R. P. *Eng. Sci.* **1960**, *23*, 22.
(2) von Hippel, A. R. *Science* **1962**, *138*, 91.
(3) Drexler, K. E. *Proc. Natl. Acad. Sci. U.S.A.* **1981**, *78*, 5275.
(4) Drexler, K. E. *Engines of Creation*; Doubleday: New York, 1986.
(5) Zach, M. P.; Ng, K. H.; Penner, R. M. *Science* **2000**, *290*, 2120.
(6) Joachim, C.; Gimzewski, J. K.; Aviram, A. *Nature* **2000**, *408*, 541.

(7) Chadwick, A. V. *Nature* **2000**, *408*, 925.
(8) Sata, N.; Ebermann, K.; Eberl, K.; Maier, J. *Nature* **2000**, *408*, 946.
(9) Craighead, H. G. *Science* **2000**, *290*, 1532.
(10) Quake, S. R.; Schrerer, A. *Science* **2000**, *290*, 1536.
(11) Jager, E. W. H.; Smela, E.; Inganäs, O. *Science* **2000**, *290*, 1540.
(12) Paiella, R.; Capasso, F.; Gmachi, C.; Sivco, D. L.; Baillargeon, J. N.; Hutchinson, A. D.; Cho, A. Y.; Liu, H. C. *Science* **2000**, *290*, 1739.
(13) Suenaga, K.; Tencé, M.; Mory, C.; Colliex, C.; Kato, H.; Okazaki, T.; Shinohara, H.; Hirahara, K.; Bandow, S.; Lijima, S. *Science* **2000**, *290*, 2280.
(14) Jortner, J. *Z. Phys. D* **1992**, *24*, 247.
(15) Castleman, A. W., Jr.; Bowen, K. H., Jr. *J. Phys. Chem.* **1996**, *100*, 12911.
(16) Hartke, B. *Angew. Chem., Int. Ed.* **2002**, *41*, 1468.
(17) Kroto, H. W.; Heath, H. R.; O'Brien, S. C.; Curl, R. F.; Smalley, R. E. *Nature* **1985**, *318*, 162.
(18) Kandalam, A. K.; Blanco, M. A.; Pandey, R. *J. Phys. Chem. B* **2002**, *106*, 1945.
(19) Costales, A.; Kandalam, A. K.; Franco, R.; Pandey, R. *J. Phys. Chem. B* **2002**, *106*, 1940.
(20) Belbruno, J. J. *Chem. Phys. Lett.* **1999**, *313*, 795.
(21) Taylor, T. R.; Asmis, K. R.; Xu, C.; Neumark, D. M. *Chem. Phys. Lett.* **1998**, *297*, 133.
(22) Li, R. R.; Dapkus, P. D.; Thompson, M. E.; Jeong, W. G.; Harrison, C.; Chaikin, P. M.; Register, R. A.; Adamson, D. H. *J. Appl. Phys.* **2000**, *76*, 1689.
(23) Andreoni, W. *Phys. Rev. B* **1992**, *45*, 4203.
(24) Paulus, B.; Fulde, P.; Stoll, H. *Phys. Rev. B* **1996**, *54*, 2256.
(25) Tozzini, V.; Buda, F.; Fasolino, A. *Phys. Rev. Lett.* **2000**, *85*, 4554.
(26) Tozzini, V.; Buda, F.; Fasolino, A. *J. Phys. Chem. B* **2001**, 105, 12477.
(27) Pattanayak, J.; Kar, T.; Scheiner, S. *J. Phys. Chem. A* **2002**, *106*, 2970.
(28) Blase, X.; de Vita, A. J.; Charier, C.; Car, R. *Appl. Phys. Lett.* **1999**, *80*, 1666.
(29) Jensen, F.; Toftlund, H. *Chem. Phys. Lett.* **1993**, *201*, 89.
(30) Seifert, G.; Fowler, P. W.; Mitchell, D.; Porezag, D.; Frauenheim, Th. *Chem. Phys. Lett.* **1997**, *268*, 252.
(31) Wu, H. S.; Cui, X. Y.; Qin, X. F.; Strout, D. L.; Jiao, H. *J. Mol. Model.* **2006**, *12*, 537.
(32) Matxain, J. M.; Ugalde, J. M.; Towler, M. D.; Needs, R. J. *J. Phys. Chem. A* **2003**, *107*, 10004.
(33) Strout, D. L. *Chem. Phys. Lett.* **2004**, *383*, 95.
(34) Alexandre, S. S.; Mazzoni, M. S. C.; Chacham, H. *Appl. Phys. Lett.* **1999**, *75*, 61.
(35) Oku, T.; Nishiwaki, A.; Narita, I. *Sci. Technol. Adv. Mater.* **2004**, 1.
(36) Oku, T.; Nishiwaki, A.; Narita, I.; Gonda, M. *Chem. Phys. Lett.* **2003**, *380*, 620.
(37) Wu, H. S.; Xu, X. H.; Zhang, F. Q.; Jiao, H. *J. Phys. Chem. A* **2003**, *107*, 6609.
(38) Wu, H. S.; Jiao, H. *Chem. Phys. Lett.* **2004**, *386*, 369.
(39) Oku, T.; Nishiwaki, A.; Narita, I. *Solid State Commun.* **2004**, *130*, 171.
(40) Oku, T.; Nishiwaki, A.; Narita, I. *Physica B* **2004**, *531*, 184.
(41) Barone, V.; Koller, A.; Scuseria, G. E. *J. Phys. Chem. A* **2006**, *110*, 10844.
(42) Matxain, J. M.; Fowler, J. E.; Ugalde, J. M. *Phys. Rev. A* **2000**, *61*, 512.
(43) Hamad, S.; Catlow, C. R. A.; Spano, E.; Matxain, J. M.; Ugalde, J. M. *J. Phys. Chem. B* **2005**, *109*, 2703.
(44) Pokropivny, A. V. *Diamond Relat. Mater.* **2006**, *15*, 1492.
(45) Batsanov, S. S.; Blohina, G. E.; Deribas, A. A. *Zh. Strukt. Khim.* **1965**, *6*, 227.
(46) Pokropivny, V. V.; Pokropivny, A. V.; Skorokhod, V. V.; Kurdyumov, A. V. *Dopov. Akad. Nauk. Ukr.* **1999**, *4*, 112.
(47) Hohemberg, P.; Kohn, W. *Phys. Rev.* **1964**, *136*, B864.
(48) Becke, A. D. *J. Chem. Phys.* **1993**, *98*, 5648.
(49) Lee, C.; Yang, W.; Parr, R. G. *Phys. Rev. B* **1988**, *37*, 785.
(50) Adamo, C.; Barone, V. *J. Chem. Phys.* **1998**, *108*, 664.
(51) Gilbert, T. M. *J. Phys. Chem. A* **2004**, *108*, 2550.
(52) LeTourneau, H. A.; Birsch, R. E.; Korbeck, G.; Radkiewicz-Poutsma, J. L. *J. Phys. Chem. A* **2005**, *109*, 12014.
(53) Möller, C.; Plesset, M. S. *Phys. Rev.* **1934**, *46*, 618.
(54) Ovcharenko, I.; Aspuru-Guzik, A.; Lester, W. A., Jr. *J. Chem. Phys.* **2001**, *114*, 7790.
(55) Frisch, M. J.; Trucks, G. W.; Schlegel, H. B.; Scuseria, G. E.; Robb, M. A.; Cheeseman, J. R.; Montgomery, J. A., Jr.; Vreven, T.; Kudin, K. N.; Burant, J. C.; Millam, J. M.; Iyengar, S. S.; Tomasi, J.; Barone, V.; Mennucci, B.; Cossi, M.; Scalmani, G.; Rega, N.; Petersson, G. A.; Nakatsuji, H.; Hada, M.; Ehara, M.; Toyota, K.; Fukuda, R.; Hasegawa, J.; Ishida, M.; Nakajima, T.; Honda, Y.; Kitao, O.; Nakai, H.; Klene, M.; Li, X.; Knox, J. E.; Hratchian, H. P.; Cross, J. B.; Bakken, V.; Adamo, C.; Jaramillo, J.; Gomperts, R.; Stratmann, R. E.; Yazyev, O.; Austin, A. J.; Cammi, R.; Pomelli, C.; Ochterski, J. W.; Ayala, P. Y.; Morokuma, K.; Voth, G. A.; Salvador, P.; Dannenberg, J. J.; Zakrzewski, V. G.; Dapprich, S.; Daniels, A. D.; Strain, M. C.; Farkas, O.; Malick, D. K.; Rabuck, A. D.; Raghavachari, K.; Foresman, K.; Ortiz, J. V.; Cui, Q.; Baboul, A. G.; Clifford, S.; Cioslowski, J.; Stefanov, B. B.; Liu, G.; Liashenko, A.; Piskorz, P.; Komaromi, I.; Martin, R. L.; Fox, D. J.; Keith, T.; Al-Laham, M. A.; Peng, C. Y.; Nanayakkara, A.; Challacombe, M.; Gill, P. M. W.; Johnson, B.; Chen, W.; Wong, M. W.; Gonzalez, C.; Pople, J. A. Gaussian 03, Revision C.02; Gaussian, Inc.: Wallingford, CT, 2004.
(56) Soler, J. M.; Artacho, E.; Gale, J. D.; García, A.; Junquera, J.; Ordejón, P.; Sánchez-Portal, D. *J. Phys.: Condens. Matter* **2002**, *14*, 2745.
(57) Perdew, J. P.; Burke, K.; Ernzerhof, M. *Phys. Rev. Lett.* **1996**, *77*, 3865.
(58) Troullier, N.; Martins, J. L. *Phys. Rev. B* **1991**, *43*, 1993.
(59) Kleinman, L.; Bylander, D. M. *Phys. Rev. Lett.* **1982**, *48*, 1425.
(60) Monkhorst, H. J.; Pack, J. D. *Phys. Rev. B* **1973**, *13*, 5188.